Modelling and Simulation of the Expansion of a Shape Memory Polymer Stent

Ruoxuan Liu[†], Sean McGinty[*], Fangsen Cui[‡], Xiaoyu Luo[#] and Zishun Liu[†©]

[†] Inter. Center for Applied Mechanics, State Key Laboratory for Strength and Vibration of Mechanical Structures, Xi'an Jiaotong University, Xi'an, 710049, China.

[*] Division of Biomedical Engineering, University of Glasgow, G12 8QQ, UK.

[‡] Institute of High Performance Computing, A*STAR, Singapore 138632.

[#] School of Mathematics & Statistics, University of Glasgow, Glasgow, G12 8SQ, UK.

Abstract

Purpose – The purpose of this paper is to demonstrate the feasibility of using SMP for developing vascular stent. In particular the expansion performance is analyzed through extensive modeling and simulation.

Design/methodology/approach –Firstly, we construct the model geometry and propose a constitutive model to describe the deformation of the stent due to the expansion process. We then simulate the expansion process under varying conditions, including different heating rates and recovery temperatures. Finally, we analyze the radial strength of the SMP stent.

Findings –A less invasive and stable expansion performance of the SMP stent is confirmed by the simulation method. A fitting function of the expansion process is proposed based on the characteristics of the SMP.

Research limitations/implications – The effects of dynamic blood flow on the SMP stent is ignored. A fluid-structure interaction analysis may need to be considered to give a more accurate description of the behavior of the SMP stent.

Social implications – Our findings will provide guidance for the rational design and application of SMP stents.

Originality/value – This is the first time that the expansion performance of a SMP stent has been analyzed qualitatively and quantitatively through modelling and simulation.

Keywords Shape memory polymer stent (SMP stent), expansion performance, Modelling and simulation

Paper type Research paper

1. Introduction

Nowadays, cardiovascular disease is one of the most dangerous diseases in the world. Applying stents into narrowed blood vessels to restore normal blood flow is a less invasive method for the treatment of cardiovascular diseases (Neamtu *et al*., 2014, Ravindranath *et al*., 2015, Kuribayashi *et al*., 2006, Layman *et al*., 2010). Traditional materials for medical stents are stainless steel, nickel titanium alloy or cobalt chromium alloy. However, the contact between metal stent and vascular wall initiates a biological response that causes intimal hyperplasia and restenosis of the blood vessel. In addition, inflammation and thrombosis are side effects which have been associated with lack of biocompatibility of metal materials (Wang *et al*., 2016). To improve the performance of cardiovascular stents, shape memory polymers (SMPs) have been suggested as a new potential material (Hou *et al*., 2016).

SMPs, as a new type of smart material (Zheng *et al*., 2018, Rosso *et al*., 2005, Z. Liu *et al*. 2015, Eskandari et al. 2018), have superior large deformation characteristics, good biocompatibility and biodegradability (Liu *et al*., 2007, Ratna and Karger-Kocsis, 2008). They therefore represent a good candidate material to address limitations associated with more traditional materials like metals. Examples of the current use of SMPs include SMP scaffolds (Lendlein and Langer, 2002). Compared with traditional steel stents, SMP stents exhibit good stiffness compatibility with the vessel and tunable deformation for navigating highly tortuous vessels (Small *et al*., 2010). Many investigations have already been reported on the feasibility of SMP stents. Wache et al. proposed a new concept for a vascular endoprothesis stent made by SMPs and discussed the possibility of using the stent as a drug delivery system (Wache *et al*., 2003). Gall et al. explored the shape memory effect in polymer networks intended for cardiovascular applications (Gall *et al*., 2010). Yackacki et al. proposed the use of SMPs for cardiovascular stent interventions to reduce the catheter size for delivery (Yakacki *et al*., 2007). The SMP stent offered highly controlled and tailored deployment at body temperature. Baer et al. showed the design and fabrication of an SMP stent and a means of light delivery for photothermal actuation (Baer *et al*., 2007, Baer *et al*., 2009). Ajili et al. in an experimental study proposed a polyurethane/polycaprolactone (PU/PCL) blend as a material for SMP stents (Ajili *et al*., 2009). Although the experiments showed good biocompatibility and biodegradability of SMP scaffolds, a theoretical and numerical study on the whole deformation behavior has been lacking.

During deployment, stents are delivered to the diseased artery in a crimped state and are then expanded, usually through balloon inflation. In contrast, the SMP stent would expand initiatively by temperature stimuli. In previous study, the numerical analysis of SMP stents is most concentrated on the compressive behavior (Kim *et al*., 2010), while the crucial expansion properties are ignored. Therefore, existing numerical studies do not account for the complete deployment process. Modelling and simulation has the potential to help fully understand the detailed deformation behavior and the effects of SMP stent recovery

parameters on the SMP stent deformation. Furthermore, a clearly defined analysis method should be proposed to give a concrete and characteristic description of the SMP stent.

In the present work, we adopt a numerical modelling and simulation approach to investigate the feasibility and design aspects of SMP stent expansion. Unfortunately, previous attempts to provide constitutive relationships for SMP stents have not accounted for the possibility of large deformation of the SMP stent. Hence, a modified constitutive model able to describe large deformation and more accurately capture the expansion process will be considered here. Besides, the detailed expansion performance of SMP stent is investigated. Differently from traditional metal stents, the expansion of SMP stents is spontaneous due to the properties of SMPs and is influenced by many factors, such as heating rate and recovery temperature. In the following work, the effects of heating rate and recovery temperature on the expansion of SMP stents will be studied. In addition, the radial strength of the SMP stent is also analyzed. Moreover, a fitting equation based on the characteristics of shape memory polymer is proposed to describe the SMP stent expansion routine.

The paper is organized as follows. Section 2 describes the geometric models of the stent and the blood vessel. The material constitutive models of the stent, plaque and vessel are also discussed. Considering the longitudinal strength of the stent, a parallel structure is chosen to analyze the thermomechanical performance. Section 3 outlines the numerical computation of the SMP stent expansion. In this section, the effect of heating rate and temperature is assessed. The numerical results are discussed in section 4. We also compare the results with shape memory alloy stents and find the SMP stent to be more stable. Finally, we make a summary of the numerical performance of the SMP stent.

2. Modelling of SMP stent, plaque and vessel

2.1 Geometric models

The structure of vascular stents has evolved with time to overcome limitations associated with earlier designs. The geometry of the stent is a critical factor to ensure an adequate expansion process. Nowadays, the popular structure for metal stents is a ring with a link (series stent), in order to get a better longitudinal compliance for the high modulus of metal. However, the SMP stent is much softer than metal by an order of magnitude at “MPa” and the SMP stent may not provide enough radial strength if designed in the same way as metal stent, as SMPs are much softer than metals. Thus, we should reconsider the structure of SMP stents. Wang et al. discussed four geometrical families of stent: individual stents, series stents, parallel stents and series–parallel stents (Wang *et al*., 2017). They considered the ability of the stent to resist deformation induced by outer pressure, what they referred to as resistive force (RF) in their paper. The comparison of resistive force of the four stents showed that the series–parallel stent exhibited the largest resistive force under a compression constraint. Therefore, we adopt the series–parallel structure to demonstrate the thermo-mechanical behavior of the SMP stent (Figure 1). The model is composed of a periodic arrangement of cells, specifically twelve cells in both the circumferential and longitudinal directions. The model of the vessel with idealized plaque is shown in Figure 2. We consider idealized cylindrical vessel and plaque geometries in this preliminary study. The specific geometric parameters including diameter, thickness and length of the expansion model are listed in Table 1. In order to enable vessel expansion, the diameter of the SMP stent is larger than that of the vessel. The thickness of plaque is varied as 0.2, 0.4 and 0.6mm to represent different stenosis. The stenosis

represents the reduction area of vessel. For the thickness of 0.2, 0.4 and 0.6mm, the corresponding stenosis rate is 9.3%, 19.95% and 32.25% respectively. Later we will discuss the expansion properties of the SMP stent at different levels of stenosis.

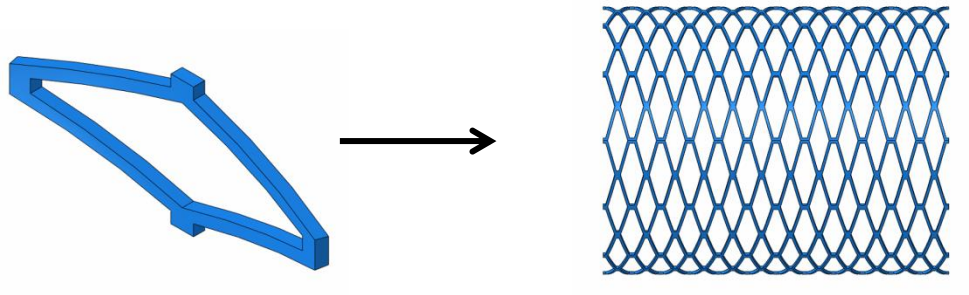

Figure 1. The 3D model of SMP stent

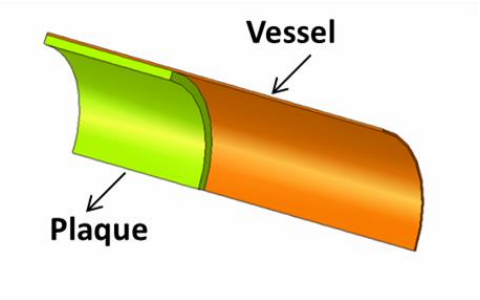

Figure 2. Schematic of the idealized geometry showing one eighth of a 3D model of the vessel with stenosis

Table 1. The geometric parameters of the vessel, plaque and SMP stent

	Outer Diameter(mm)	Thickness(mm)	Length(mm)
Vessel	9.4	0.1	20
Plaque	9.2	0.2/0.4/0.6	6
SMP stent	10.6	0.1	6.8

2.2 Constitutive models

Many different constitutive models have been proposed to accurately describe the thermomechanical behavior of SMP materials in a variety of applications (Li *et al*., 2015, Li *et al*., 2017, Li and Liu, 2018, Pan and Liu, 2018). However, most constitutive models are restricted on describing a large deformation of SMPs or explaining the large deformation with a complex expression. For example, Liu et al. proposed a rheological constitutive model using the concept of "frozen phase" and "active phase" (Liu *et al*., 2006). The model quantified the storage and release of the entropic deformation during the shape memory process under a small strain of 10%. A nonlinear constitutive model developed by Tobushi et al. could describe the thermo-mechanical properties of a higher 20% strain level (Tobushi *et*

al., 2001). However, the constitutive equation involved many coefficients being dependent on time or temperature. To enable the possibility of allowing for large deformations of the SMP stent, we adopt our model established by He et al. to show the thermo-mechanical behavior of SMP (He *et al*., 2015). The model is composed of a series of generalized Maxwell elements and a hyperelastic component (Figure 3).

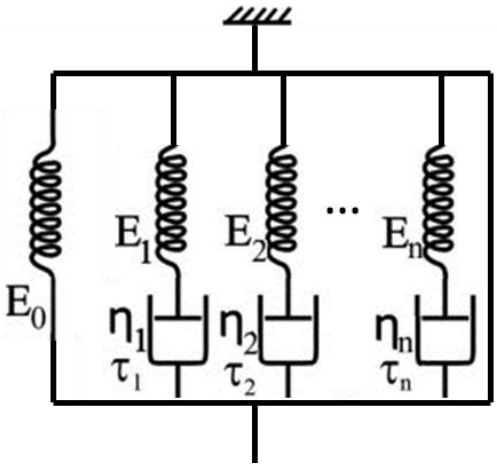

Figure 3. Schematic of generalized Maxwell model.

The constitutive equation can be derived as:

$$\sigma(t) = E_0\varepsilon_0 + \varepsilon_0 \sum_{i=1}^{n} E_i e^{-t/\tau_i} \quad (1)$$

where $\sigma(t)$ is the total stress, E_0 is the Young's modulus of the elastic item, ε_0 is the strain of the model, t is the real time, E_i and τ_i are the Young's modulus and relaxation time of the Maxwell element. n is number of Maxwell elements.

The generalized Maxwell model represents the viscoelasticity and WLF (Williams-Landel-Ferry) equation shows the relationship of time and temperature. Using the experimental data in Diani et al., the model has already been shown to be reliable under large deformation conditions (Diani *et al*., 2012). In the generalized Maxwell model, the relaxation moduli $G(t)$ can be expressed in form of a Prony series:

$$G(t) = G_\infty + \sum_{i=1}^{n} G_i \cdot e^{-t/\tau_i} \quad (2)$$

where G_∞ is the shear moduli at the infinite time. Gi is shear moduli of Maxwell element.

The coefficients can be derived from dynamic mechanical analysis experiments of the SMP by Fourier transformation. The relaxation moduli can be written by storage modulus and loss modulus:

$$G(\omega)^2 = G_s(\omega)^2 + G_l(\omega)^2 \quad (3)$$

$$G_s(\omega) = G_0 + \sum_{i=1}^{n} \frac{G_i \tau_i{}^2 \omega^2}{1+\tau_i{}^2\omega^2} \quad (4)$$

$$G_l(\omega) = \sum_{i=1}^{n} \frac{G_i \tau_i \omega}{1+\tau_i{}^2\omega^2} \quad (5)$$

where $G_s(\omega)$ is storage modulus and $G_l(\omega)$ is loss modulus, ω is the frequency during dynamic mechanical testing. To get a more accurate description of storage and loss modulus, the n is set as 12. Based on the results of Diani et al. (Diani *et al*., 2012), the series of G_i , τ_i

and G_0 can be obtained with WLF equation. G_0 is 1.6MPa. The specific values of G_i and τ_i are listed in Table 2.

Table 2. Generalized Maxwell model relaxation times and associated shear moduli pairs

$G_i(Pa)$	0.1476×10^9 0.1756×10^9 0.2025×10^9 0.1775×10^9 0.6802×10^8 0.1139×10^8
$\tau_i(s)$	0.3031×10^{-4} 0.1721×10^{-3} 0.9768×10^{-2} 0.5545×10^{-2} 0.3147×10^{-1} 0.1787
$G_i(Pa)$	0.2264×10^7 0.8132×10^6 0.4020×10^6 0.1760×10^6 0.5056×10^5 0.1265×10^5
$\tau_i(s)$	0.1014×10^1 0.5757×10^1 0.3268×10^2 0.1855×10^3 0.1053×10^4 0.5977×10^4

The WLF equation can be written as:

$$lg(\alpha_T) = \frac{-C_1(T-T_r)}{C_2+T-T_r} \tag{6}$$

where α_T is the time-temperature superposition shifting factor, C_1 and C_2 are material constants and T_r is the reference temperature. By fitting the stress relaxation curve at different temperatures *T* (Diani *et al*., 2012), we can obtain that C_1=10.17, C_2=47.35℃ and T_r is 50℃.

In addition, a hyperelastic term (instead of an elastic term) is added to enable better agreement due to the large strain of the SMP stent. Here, we choose a Neo-Hookean hyperelastic equation:

$$U = C_{10} \cdot (I_1 - 3) + \frac{1}{D_1} \cdot (J_{el} - 1)^2 \tag{7}$$

where U is the strain energy density, I_1 is the first strain invariant, $\mathrm{J_{el}}$ is the elastic volume strain, $\mathrm{C_{10}} = \mathrm{G'}/2$ and $\mathrm{D_1} = 2/\mathrm{K'}$. The parameters $\mathrm{G'}$ and $\mathrm{K'}$ are the initial shear modulus and bulk modulus, respectively, at initial time. In this paper, the $\mathrm{K'}$ is considered as a constant of 3.1GPa. Make the time as zero, we can get that $G' = G_\infty + \sum_{i=1}^{12} G_i$. Therefore, the coefficients $\mathrm{C_{10}}$ and $\mathrm{D_1}$ can be obtained as 393.964 and 0.0006452 MPa.

For the vessel and plaque materials, we adopt the polynomial-form hyperelastic model proposed by Migliavacca et al. (Migliavacca *et al*., 2004, Migliavacca *et al*., 2007) which has been shown to be a good description of the mechanical behavior of vessel and plaque. For the vessel, the constitutive equation is written as:

$$U = C_{10} \cdot (I_1 - 3) + C_{03} \cdot (I_2 - 3)^3 \tag{8}$$

I_1 and I_2 are the first and second strain invariant. The coefficients C_{10} and C_{03} are 0.019513 and 0.02976 MPa. For the plaque, the constitutive equation is written as:

$$U = C_{10} \cdot (I_1 - 3) + C_{02} \cdot (I_2 - 3)^2 + C_{03} \cdot (I_2 - 3)^3 \tag{9}$$

The coefficients $\mathrm{C_{10}}$, $\mathrm{C_{02}}$ and $\mathrm{C_{03}}$ are 0.04, 0.003 and 0.02976 MPa, respectively.

The geometrical models and constitutive equations were implemented within commercial software (ABAQUS), allowing us to perform simulations of the SMP stent expansion under different conditions.

3. Simulation of the expansion process of the SMP stent

SMPs can recover their original shape under a stimulus such as heat, light or a magnetic field. In this work we choose a thermal motivated SMP and the SMP stent can be activated by laser. The work process of an SMP stent can be divided into four steps: compress the stent to a small geometry under a high temperature (T>Tg); then retain the deformation and cool the stent (T>Tg); release the load and deliver the stent to the target disease position; finally increase the temperature to the programmed temperature and then cool the stent to body temperature. The deformation process is shown in Figure 4.

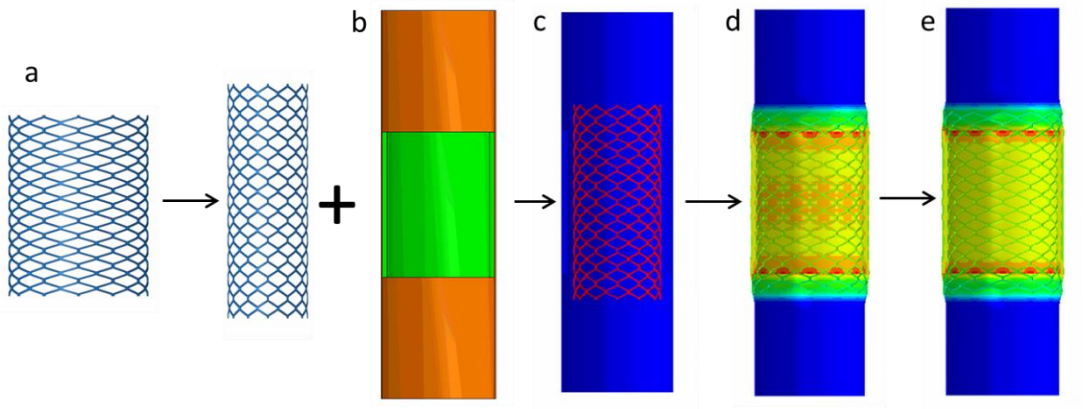

Figure 4. The work process of the SMP stent: (a) original state of the SMP stent, (b) the compressed stent entering into the vessel, (c) shrunk stent in programmed location of vessel, (d) SMP stent expanding the stenosis, (e) SMP stent reaching force equilibrium with vessel

We already know that the recovery temperature, recovery time and heating rate can influence the free recovery of the SMP (Yu, *et al*., 2014). Therefore, to make the expansion of SMP stent more programmable, the effect of heating rate and recovery temperature should be understood. In this paper, three heating rates and four recovery temperatures are designed. With a fixed stenosis of 19.95% and recovery temperature of 50℃ (Tg), the heating rate is varied from 3.75℃/min to 7.5℃/min and finally 15℃/min. Then, we fix the heating rate to 7.5℃/min and vary the recovery temperature from 48℃ to 50℃, 52℃and 54℃. After the heating process, the temperature is cooled down to 37℃ (body temperature) with the same cooling rate.

For the application of a given stent, the strength and compliance properties should be considered and evaluated. The radial strength S_r represents the ability to resist the deformation induced by outer pressure. It can be defined as:

$$S_r = \frac{P}{\alpha_r} = \frac{P}{\Delta U/R} \tag{10}$$

Where P is the pressure, α_r is the radial deformation ratio of stent, ΔU is the displacement of stent in radial direction and R is the radius of stent. For the calculation of circumferential tension, the pressure of stent is inhomogeneous during expansion. We assume a homogeneous pressure P_0 on the contact plaque to replace of the inhomogeneous pressure. Thus, the circumferential force, f_p can be derived as :

$$f_p = P_0 \cdot l_p \cdot R_p \tag{11}$$

where l_p and R_p are the length and radius of the plaque.

For a half model of the expanded plaque (Figure 5), the total force induced by contact pressure is equal to the force acting on the two ends of the symmetry. Thus, the force balance is written as:

$$2l_p R_p P_0 = 2F = 2\sum_{i=1}^{n} \sigma_i s_i \tag{12}$$

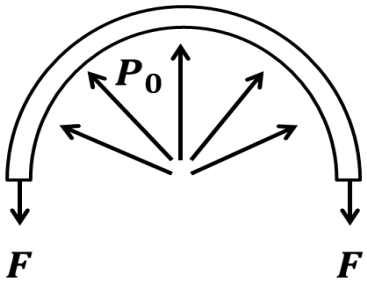

Figure 5. The schematic diagram of force acting on the half plaque

Where i is the number of the elements of end of half model, σ_i is the normal stress of the element and s_i is the deformed area of the element. Therefore, the circumferential tension is derived as:

$$f_p = \sum_{i=1}^{n} \sigma_i s_i \tag{13}$$

The radial strength is

$$S_r = \frac{\sum_{i=1}^{n} \sigma_i s_i}{l_p R_p \Delta U / R} \tag{14}$$

4. Results and discussion

Through the implementation of the geometric models and constitutive theory of the SMP stent, plaque and vessel into commercial software (ABAQUS), we obtain the expansion performance of the SMP stent in different recovery conditions. We first simulate the expansion of the SMP stent at different levels of stenosis. Then, the effect of heating rate and recovery temperature is investigated. Finally, the radial strength is discussed.

4.1 Vessel expansion under different conditions

4.1.1 Vessel expansion under different levels of stenosis

The SMP stent was heated to 50℃with a constant heating rate of 3.75℃/min. The radius of the stent and plaque during expansion can be seen as in Figure 6. With temperature increasing to 50℃, the radius of stent rapidly increases and tends towards a fixed value after cooling down. Correspondingly, the radius of the lumen increases and the stenosis is relieved. To show the expansion effect more intuitively, a dimensionless parameter α is defined as the ratio of the displacement of stenosis in radial direction with the original thickness (as shown in Figure 7).

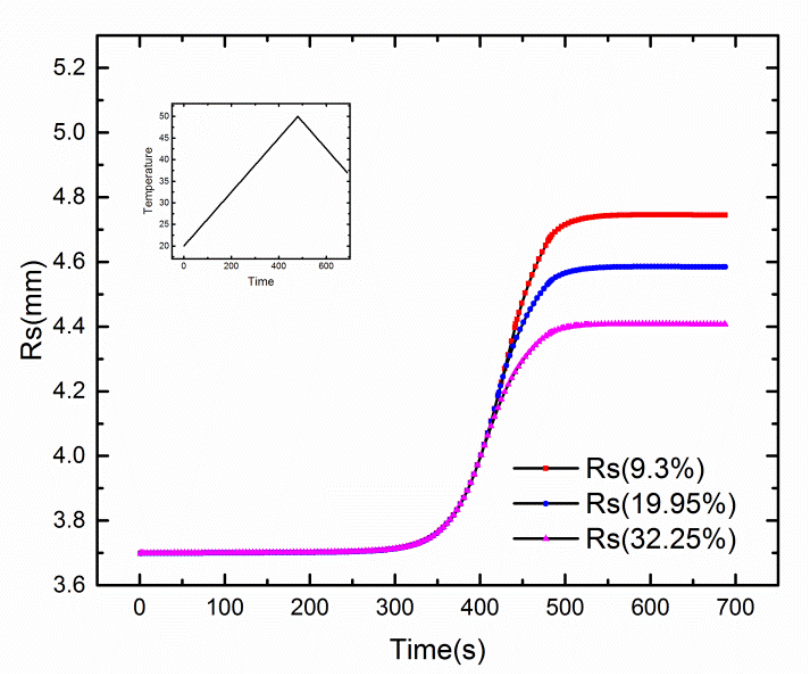

(a)

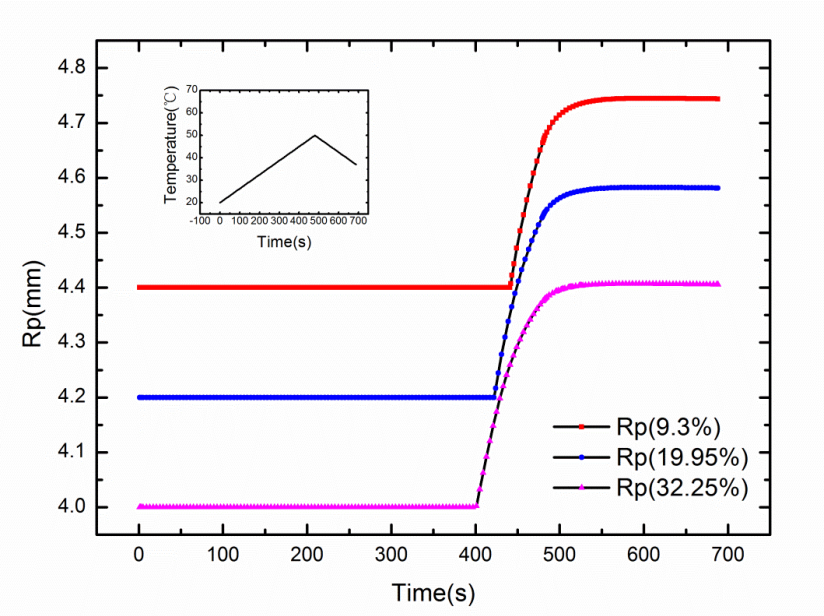

(b)

Figure 6. (a) The radius of stent during expansion under different levels of stenosis, (b) The radius of the lumen during expansion under different levels of stenosis

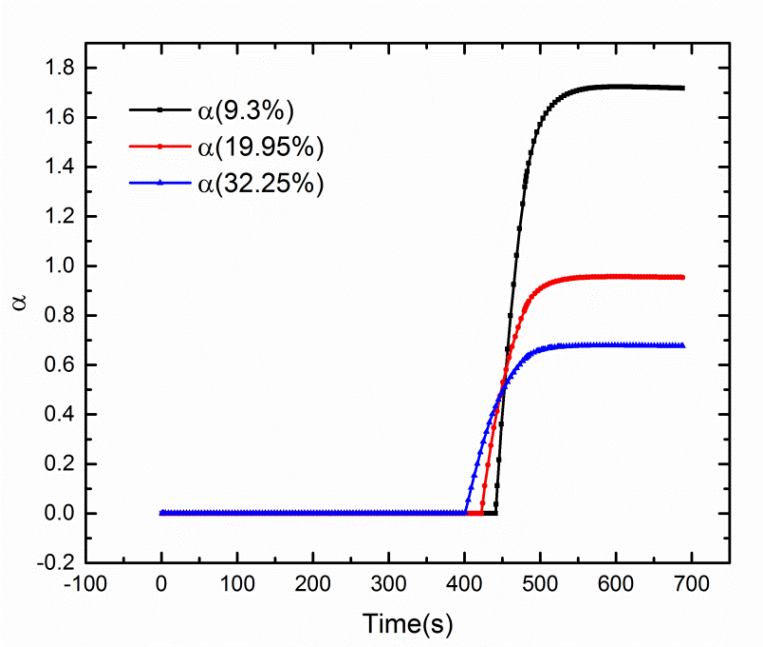

Figure 7. The ratio of the displacement of stenosis in radial direction with the original thickness.

For a stenosis of 32.25%, the thickness of plaque reduces by 60%. With a stenosis of 9.3% and 19.95%, the thickness of the plaque disappears after expansion. The stent obtains a good expansion result under the same thermal condition within 19.95% stenosis. During SMP stent expansion, the thickest plaque (32.25% stenosis) contacts with stent earlier than the 19.95% and 9.3% stenosis levels, as expected. A higher stenosis represents a higher constraint and shows a smaller decrease of radius. We define an expansion speed v as the time deferential of the recovery displacement of the stent:

$$v = \frac{dr}{dt} \tag{15}$$

The temperature where the speed reaches a maximum is defined as the characteristic recovery temperature. By analysis of the displacement of the stent, we find a smaller characteristic recovery temperature for a higher stenosis (Figure 8). In other words, a higher constraint will result in an SMP stent with a smaller characteristic recovery temperature.

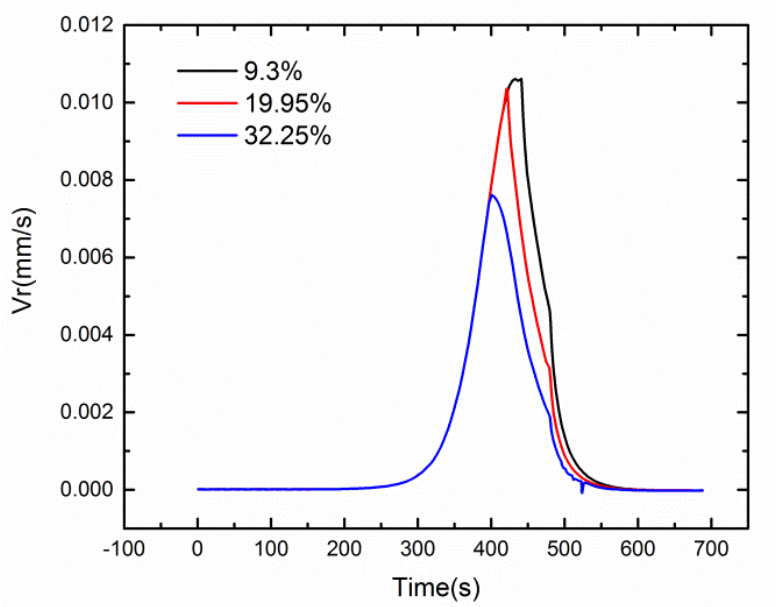

Figure 8. The expansion speed of the SMP stent

Our results demonstrate that this SMP stent model is able to expand the plaque with a good expansion performance.

4.1.2 Vessel expansion with different heating rates

The heating rate is known to influence the recovery of shape memory polymer (Yu and Qi, 2014). Here we consider the influence of heating rate on the stent expansion (in Figure 9). From Figure 9 we can see that the radius of stent and plaque increases rapidly until the temperature reaches 50℃ and becomes stable when temperature decreases to body temperature. For the same level of stenosis, an increased heating rate results in an earlier recovery which is smaller in magnitude. With the same recovery temperature, a reduced heating rate results in an increased recovery time. Thus, the stent recovers more and expands more stenosis. On the other hand, a reduced heating rate means a lower temperature at the same time. We know that the relaxation time of the polymer molecular chain is negatively related with temperature. Therefore, the visocelasticity of SMP blocks more the release of elastic strain in lower temperature and the stent recovers relatively later compared with the higher heating rate.

The results of Figure 9 show the design flexibility in terms of the expansion of the vessel with a SMP stent by varying heating rate.

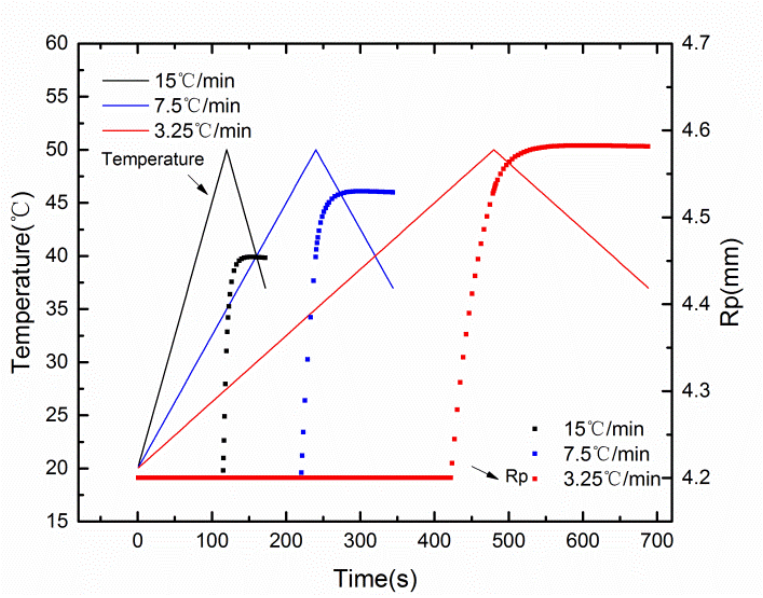

(a)

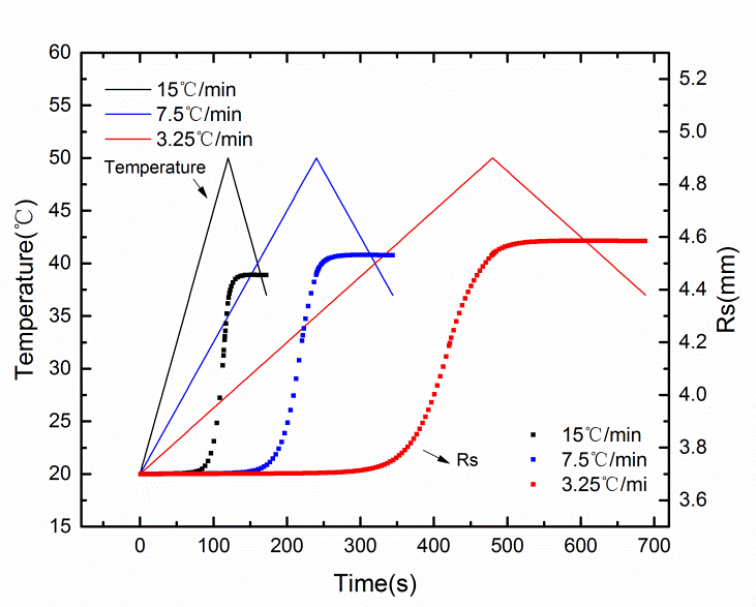

(b)

Figure 9. (a) The radius of the plaque during expansion with different heating rates, (b) The radius of the stent during expansion with different heating rates. The temperature history is also shown in the Figure.

4.1.3 Vessel expansion with different heating temperatures

Figure 10 shows the effect of recovery temperature on expansion of the SMP stent. Similarly with results in Figure 10, the radius of the SMP stent recovers rapidly with temperature increasing to the programmed temperature and then slowly grows to a stable value. It is clear that a higher recovery temperature results in a higher recovery strain.

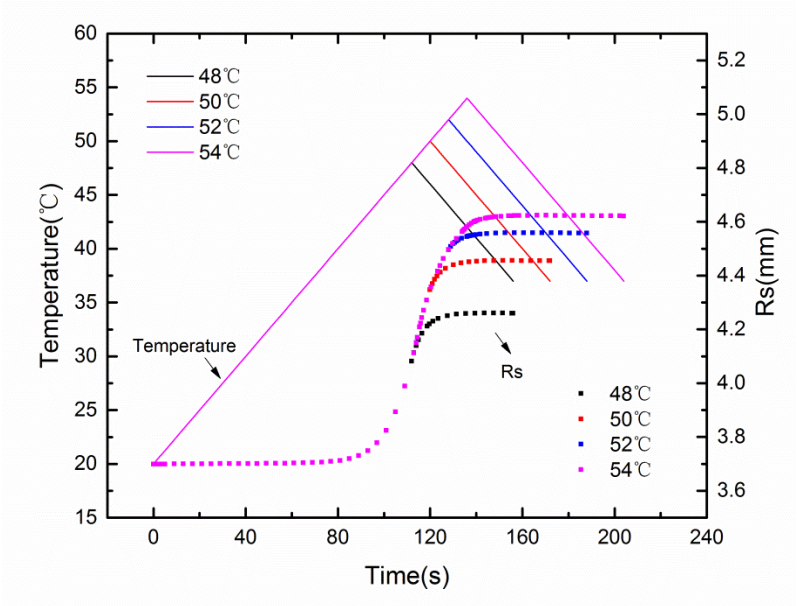

(a)

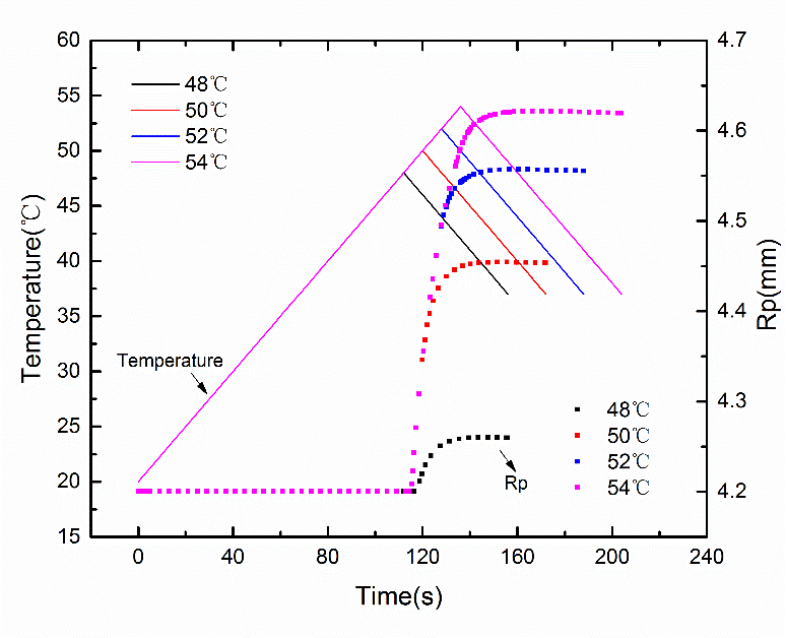

(b)

Figure 10. (a) The radius of the stent during expansion with different recovery temperatures, (b) The radius of the plaque during expansion with different recovery temperatures. The temperature history is also shown in the Figure.

In this paper, we define a fitting curve of the outer radius of the stent, R_s as the function of recovery temperature and heating rate:

$$R_s(t) = R_0(\alpha_r + \frac{1-\alpha_r}{1+e^{4(t-t_m)/\Delta t_m}}) \tag{16}$$

$$\alpha_r = \frac{R_f}{R_0} \tag{17}$$

$$\Delta t_m = R_0 \frac{1-\alpha_r}{v_{t_m}} \tag{18}$$

Where R_f is the final radius of the stent, R_0 is the compressed radius of the stent, α_r is the recovery ratio in the radial direction, t_m is the time where the slope of the radius curve reaches a maximum, Δt_m is the time span of the slope at t_m intersecting with R_0 and R_f (Figure11). The fitting results can be seen in Figure12. From equation 16 we can see that the radius is proportional to the recovery ratio α_r. From existing research on SMPs, we know that a higher recovery temperature and a smaller heating rate will introduce a higher recovery ratio, and hence a higher recovery radius of the SMP stent will be reached.

The position t_m represents the time where the expansion speed or shape recovery speed reaches the maximum during the expansion. Therefore, t_m indicates the characteristic recovery temperature. From Figure 13 (a) we see that a higher heating ratio shows a smaller characteristic recovery temperature. For different recovery temperatures with the same heating rate, a similar characteristic recovery temperature is obtained for temperatures higher than Tg (50, 52 and 54℃). A smaller characteristic recovery temperature is found for 48℃, because the phase transition is not completed at this temperature and the shape recovery speed is achieved at a smaller temperature. Therefore, using a shape recovery ratio and characteristic recovery temperature, we have shown that a smaller heating rate and a higher

recovery temperature result in a higher recovery ratio and a smaller characteristic recovery temperature, resulting in a larger recovery radius.

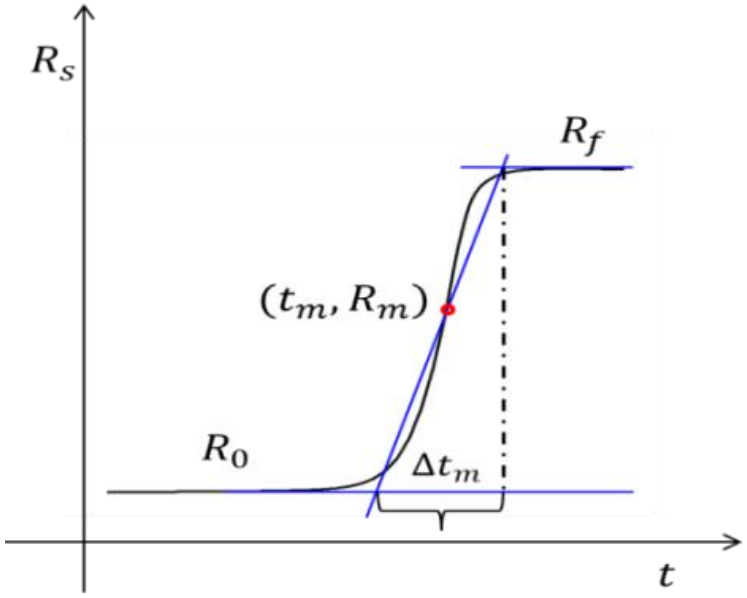

Figure 11. Schematic diagram of stent radius versus time, indicating the influence of model parameters.

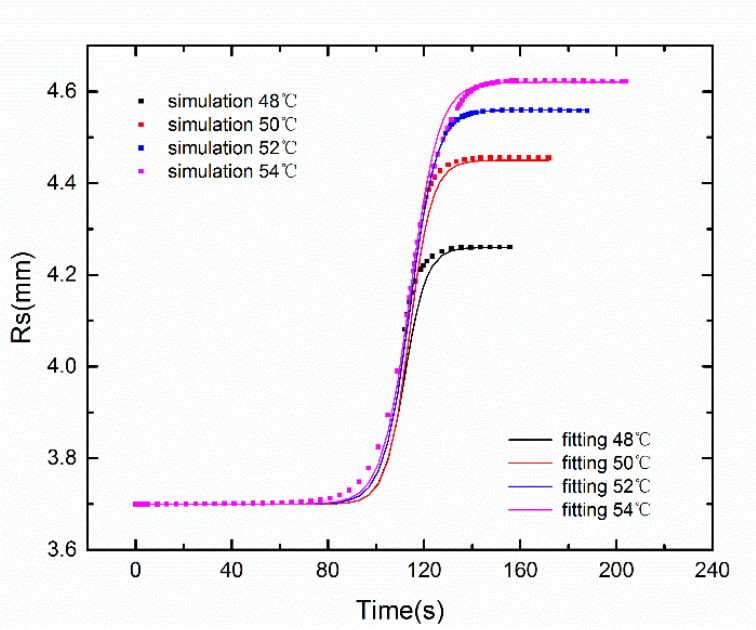

(a)

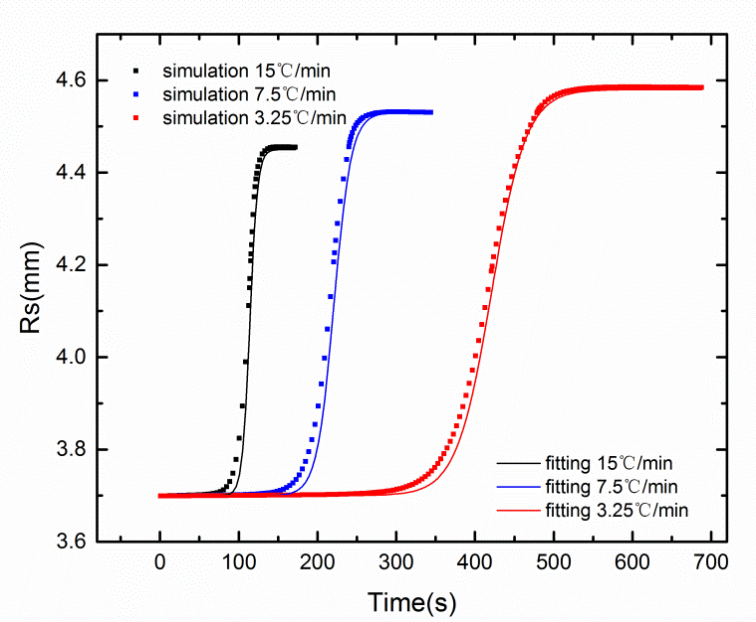

(b)

Figure 12. The fitting curve of the stent radius compared with simulation results: (a) at different recovery temperatures, (b) at different heating ratios

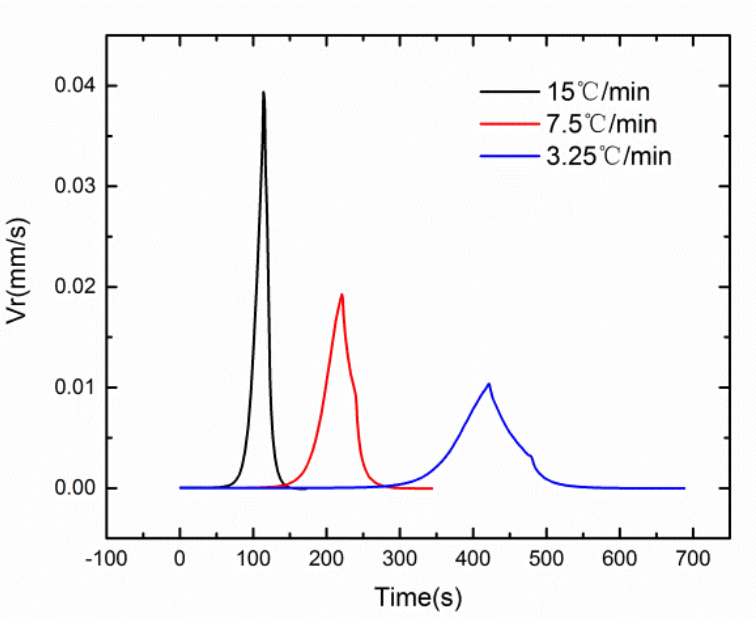

(a)

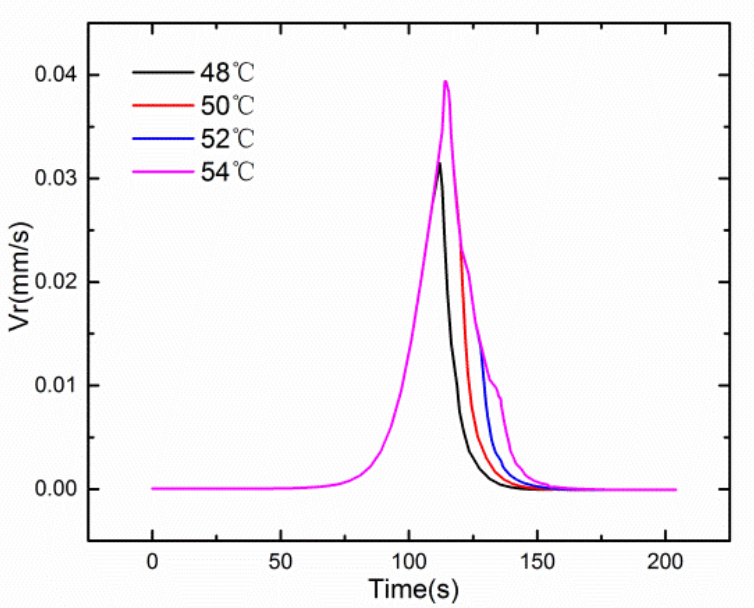

(b)

Figure 13. The expansion speed of the SMP stent: (a) at different heating rate, (b) at different recovery temperatures

The fitting curves in Figure 13 show good agreement with the simulation results. This equation will be useful in the more rational design of SMP stents, where a desired stent expansion can be programmed by varying the parameters.

4.2 The radial strength of the SMP stent

By the application of equations (13) and (14), we can obtain the circumferential force and radial strength in Figure 14 and 15. The different stenosis levels represent different constraints for the SMP stent recovery. We can see a small contact force of approximately 1.0×10^{-8} Newtons. This means the contact between the SMP stent and vessel is very soft and no damage will be caused. Figure 14 (a) shows a bigger recovery force of SMP stent to expand the larger stenosis, while a larger radial strength is observed in a smaller stenosis. It's easy to understand that a larger stenosis provides a larger constraint for SMP stent expanding and hence needs a larger recovery force. For radial strength, as shown in equation 14, the radius of the plaque is inversely related to radial strength. Thus, the radius of stent is smaller and the radial strength is bigger for a thicker plaque. The results in Figure 14 (b), (c) and Figure15 (b), (c) show that the decreasing heating rate and increasing recovery temperature can have a similar effect on the radial strength. A smaller heating rate and a higher temperature both provide a longer recovery time and lead to larger recovery strength.

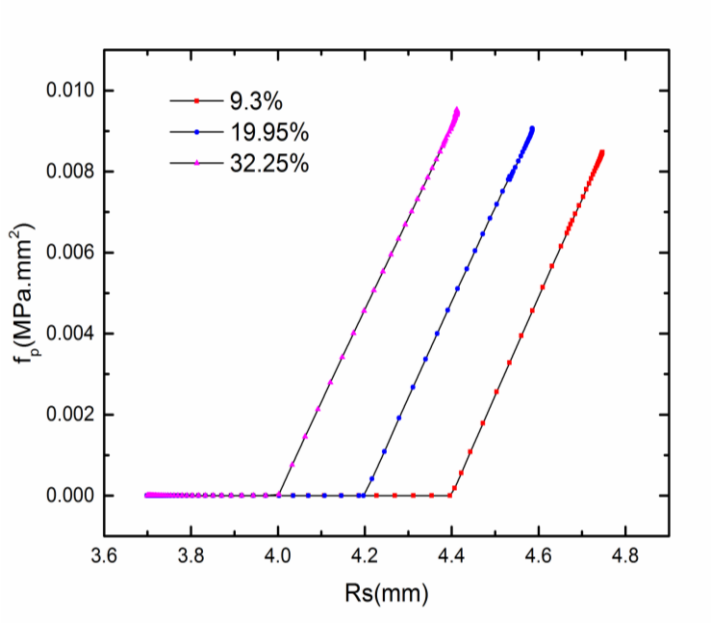
9.3%
19.95%
32.25%
0.010
0.008
0.006
0.004
0.002
0.000
3.6
3.8
4.0
4.2
4.4
4.6
4.8
f_p(MPa.mm^2)
Rs(mm)

(a)

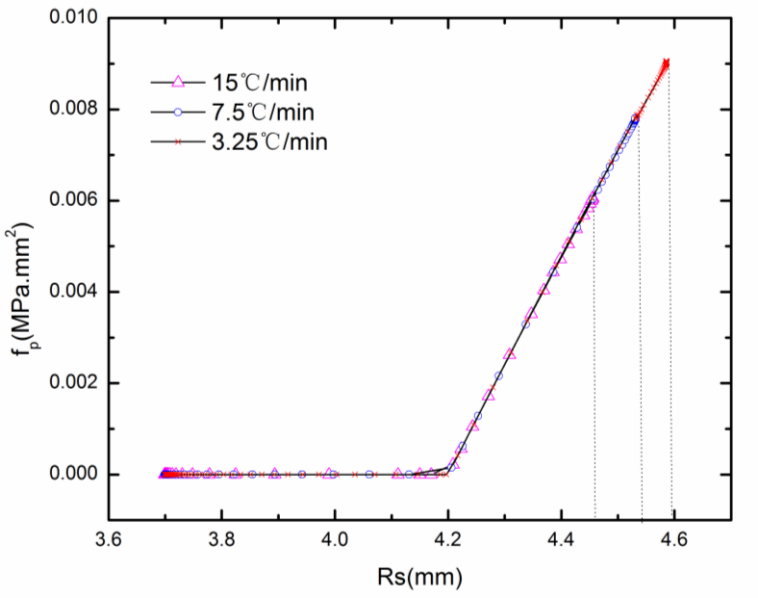
15℃/min
7.5℃/min
3.25℃/min
0.010
0.008
0.006
0.004
0.002
0.000
3.6
3.8
4.0
4.2
4.4
4.6
f_p(MPa.mm^2)
Rs(mm)

(b)

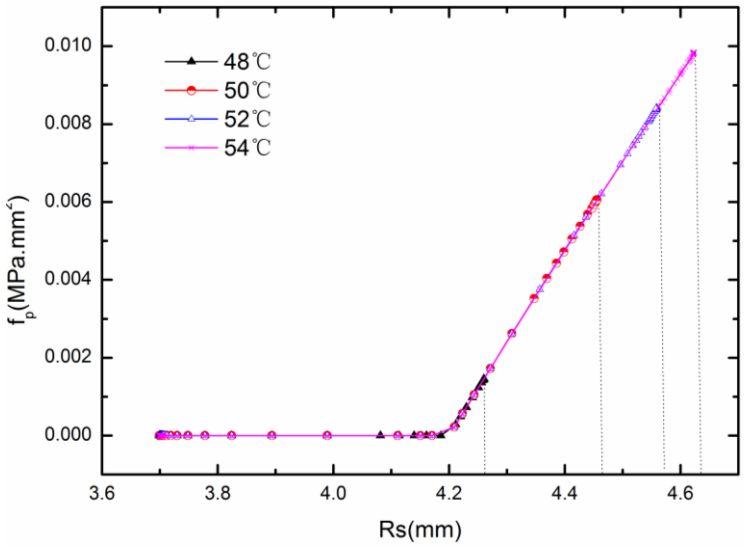
48℃
50℃
52℃
54℃
0.010
0.008
0.006
0.004
0.002
0.000
3.6
3.8
4.0
4.2
4.4
4.6
f_p(MPa.mm^2)
Rs(mm)

(c)

Figure 14. The circumferential force of the stent during expansion: (a) at different stenosis, (b) at different heating rates, (c) at different recovery temperatures

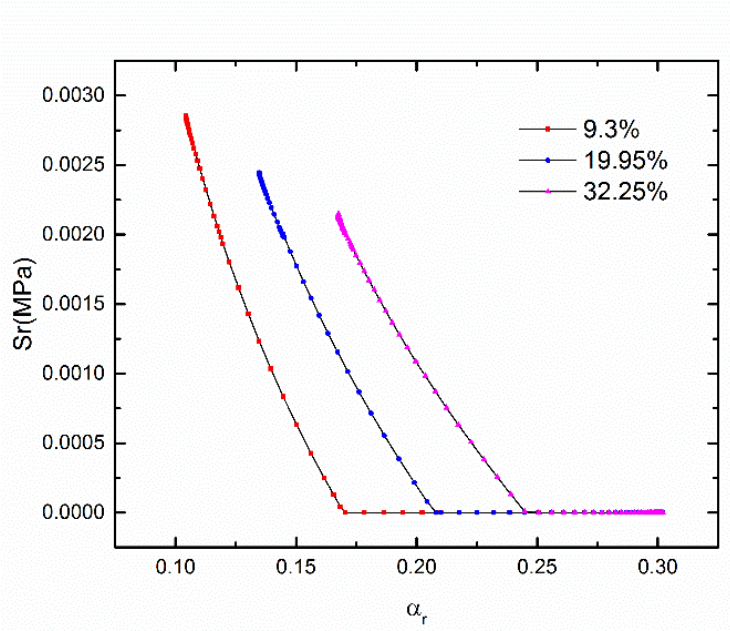

(a)

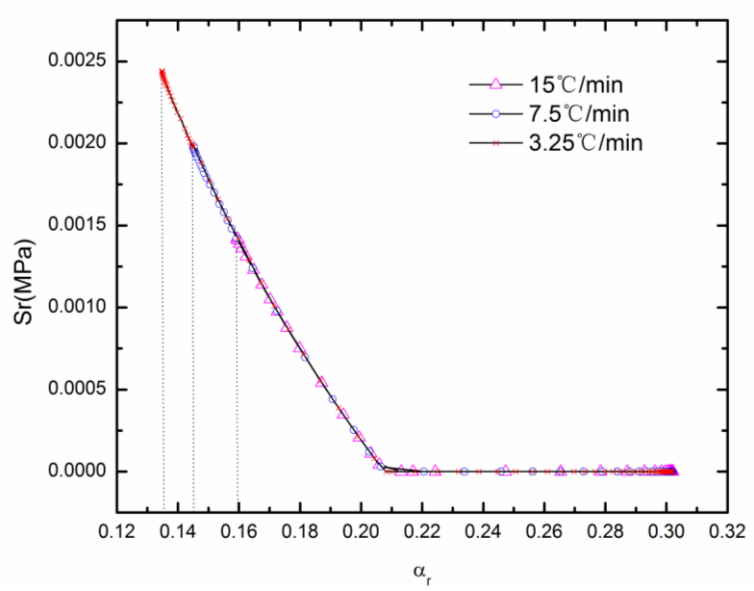

(b)

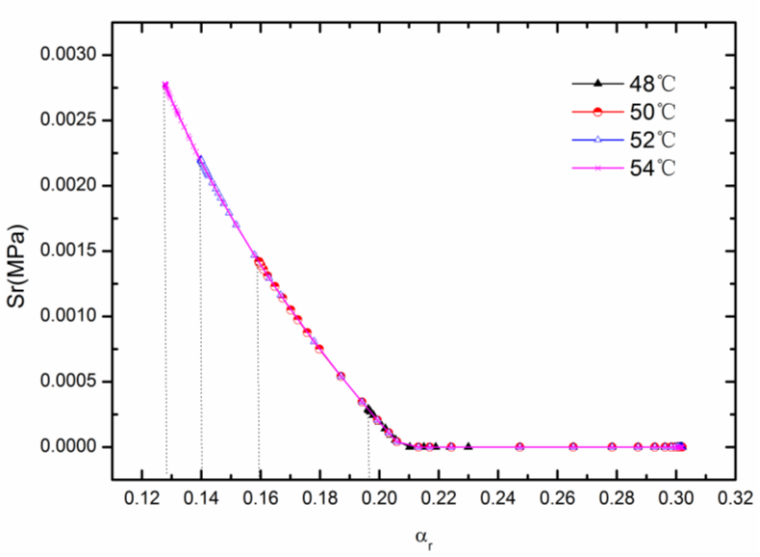

(c)

Figure 15. The radial strength of the stent during expansion: (a) at different stenosis, (b) at different heating rates, (c) at different recovery temperatures

From the results in Figure 14, we can see that the circumferential force of the SMP stent undergoes two processes. Before the contact of the SMP stent and plaque, the SMP stent recovers to its original shape freely and the circumferential force is zero. After contact, the circumferential force increases with the increase of radius of the SMP stent and finally tends towards a fixed value. To investigate the performance of SMP stent more clearly, the circumferential force evolution with temperature is shown in Figure16. We can see that the circumferential force of the SMP stent rapidly increases with temperature increasing after contact and increases slightly after cooling to body temperature before finally reaching a stable value. This result is different from the expansion routine of traditional stainless steel stent and shape memory alloy stent, which is usually expanded by external force and reinforced by the plasticity of metal finally. As we know, shape memory alloy (SMA) as a extensively investigated material (Ansari *et al*., 2018, Baghani *et al*., 2018, Lu *et al*., 2017), also possesses the shape memory ability and is widely applied to stent design. However, the expansion method for SMA stent is still dominated by external mechanical operation such as balloon expanding. According to previous study we know that for the constraint recovery induced by temperature of SMA, the modulus of SMA increases when Martensite transforms to Austensite during the constraint recovery. Correspondingly, thermal effects and phase transition both make an increase of recovery stress at constraint. The increasing recovery stress of shape memory alloys will expand the plaque, meanwhile cause damage to the vessel. Therefore, stent made of SMA is unsuitable to expand the plaque with the independent method. For the constraint recovery of the SMP, the compressive stress will increase first and

then decrease (as shown in Figure 17). This conclusion has been validated experimentally and theoretically *(*Lakhera *et al.,* 2012*,* Volk *et al*., 2011, Liu *et al*., 2006). Thermal effects and phase transition (modulus decrease) collectively result in the stress evolution. Thus, the stress increases first but decreases with increasing temperature and reaches to a stable value ultimately. Therefore, the SMP stent is superior in providing a harmless and stable expansion for vessel.

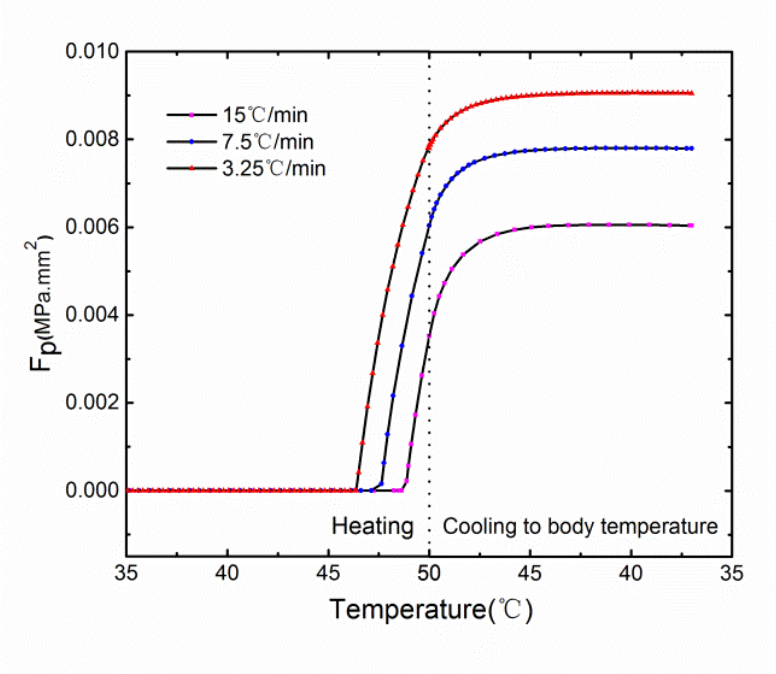

Figure 16. The circumferential force of the stent during expansion with different heating rates

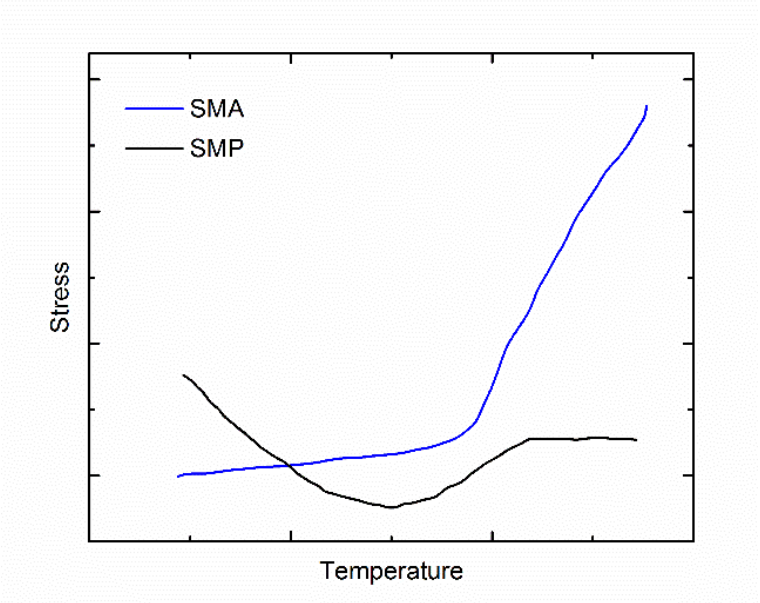

Figure 17. The schematic diagram of recovery stress evolution of SMP and shape memory alloy with a fixed constraint

5. Conclusions

In this paper, modelling and simulation of SMP stent expansion is conducted based on a combined hyperelastic and viscoelastic model. The vital expansion performance in a stenosed vessel is analyzed and discussed. The results of our simulations demonstrate that the SMP stent can obtain a soft and stable expansion performance with the human body. A higher expansion can be obtained by a smaller heating rate and larger recovery temperature. The fitting function of the recovery radius shows a good description based on the characteristic recovery ratio and recovery temperature of shape memory polymers. This paper demonstrates the feasibility to assist in the design of SMP stent using our model.

In future work, the dynamic pressure introduced by blood flow will be included within the analysis of the SMP stent. Furthermore, a strengthened SMP composite may also be considered to obtain a stronger expansion.

Acknowledgement
RXL and ZSL are grateful for the support from the National Natural Science Foundation of China through grant numbers 11811530287 and 11572236.

References

Ajili, S. H., Ebrahimi, N. G. & Soleimani, M. (2009), "Polyurethane/polycaprolactane blend with shape memory effect as a proposed material for cardiovascular implants", *Acta Biomaterialia,* Vol. 5 No**.** 5, pp. 1519-1530.

Ansari M., Fahimi P., Baghani M., and Golzar M. (2018), "An Experimental Investigation on Training of NiTi-Based Shape Memory Alloys," *International Journal of Applied Mechanics*, Vol. 10 No. 4, pp. 1850040.

Baer, G. M., Small, W., Wilson, T. S., Benett, W. J., Matthews, D. L., Hartman, J. & Maitland, D. J. (2007), "Fabrication and in vitro deployment of a laser-activated shape memory polymer vascular stent", *BioMedical Engineering OnLine,* Vol. 6 No.1, pp. 43-51.

Baer, G. M., Wilson, T. S., Ward Small, I., Hartman, J., Benett, W. J., Matthews, D. L. & Maitland, D. J. (2009), "Thermomechanical Properties, Collapse Pressure, and Expansion of Shape Memory Polymer Neurovascular Stent Prototypes", *Journal of Biomedical Materials Research Part B Applied Biomaterials,* Vol. 90B No.1, pp. 421–429.

Baghani M., Ganjiani M., and Rezaei M.. (2018), "Numerical Analysis of Growing the Ductile Damage in Structures Reinforced by SMA Using Continuum Damage Mechanics Approach," International Journal of Applied Mechanics, Vol. 10 No. 7, pp. 1850070.

Diani, J., Gilormini, P., Frédy, C. & Rousseau, I. (2012), "Predicting thermal shape memory of crosslinked polymer networks from linear viscoelasticity", *International Journal of Solids & Structures,* Vol. 49 No. 5**,** pp. 793-799.

Eskandari, A. H., Baghani M., and Sohrabpour S. (2018), "A Time-Dependent Finite Element Formulation for Thick Shape Memory Polymer Beams Considering Shear Effects," *International Journal of Applied Mechanics*, Vol. 10 No. 4, pp. 1850043.

Gall, K., Yakacki, C. M., Liu, Y., Shandas, R., Willett, N. & Anseth, K. S. (2010), "Thermomechanics of the shape memory effect in polymers for biomedical applications", *Journal of Biomedical Materials Research Part A,* Vol. 73A No. 3, pp. 339-348

He, Y., Guo, S., Liu, Z. & Liew, K. M. (2015), "Pattern transformation of thermo-responsive shape memory polymer periodic cellular structures", *International Journal of Solids & Structures,* Vol. 71**,** pp. 194-205.

Hou, L. D., Zhen, L. I., Pan, Y., Sabir, M., Zheng, Y. F. & Li, L. I. (2016), "A review on biodegradable materials for cardiovascular stent application", *Frontiers of Materials Science,*Vol. 10 No. 3**,** pp. 238-259.

Kim, J. H., Kang, T. J. & Yu, W. R. (2010), "Simulation of mechanical behavior of temperature-responsive braided stents made of shape memory polyurethanes", *Journal of Biomechanics,* Vol. 43 No. 4**,** pp. 632-643.

Kuribayashi, K., Tsuchiya, K., You, Z., Tomus, D., Umemoto, M., Ito, T. & Sasaki, M. (2006), "Self-deployable origami stent grafts as a biomedical application of Ni-rich TiNi shape memory alloy foil", *Materials Science & Engineering A,* Vol. 419 No. 1**,** pp. 131-137.

Lakhera, N., Yakacki, C. M., Nguyen, T. D. & Frick, C. P. (2012), "Partially constrained recovery of (meth)acrylate shape‐memory polymer networks", *Journal of Applied Polymer Science,* Vol. 126 No. 1**,** pp. 72-82.

Layman, R., Missoum, S. & Geest, J. V. (2010), "Simulation and probabilistic failure prediction of grafts for aortic aneurysm", *Engineering Computations,* Vol. 27 No. 1**,** pp. 84-105.

Lendlein, A. & Langer, R. (2002), "Biodegradable, Elastic Shape-Memory Polymers for Potential Biomedical Applications", *Science,* Vol. 296 No. 5573**,** pp. 1673-1676.

Li, Y. & Liu, Z. (2018), "A novel constitutive model of shape memory polymers combining phase transition and viscoelasticity", *Polymer,* Vol. 143, pp. 298-308.

Li, Y., Guo, S., He, Y. & Liu, Z. (2015), "*International Journal of Computational Materials Science & Engineering,* Vol. 4 No. 01**,** pp. 762-770.

Li, Y., He, Y. & Liu, Z. (2017), "A viscoelastic constitutive model for shape memory polymers based on multiplicative decompositions of the deformation gradient", *International Journal of Plasticity,* Vol. 91**,** pp. 300-317.

Liu, C., Qin, H. & Mather, P. T. (2007), "Review of progress in shape-memory polymers", *Journal of Materials Chemistry,* Vol. 17 No. 16**,** pp. 1543-1558.

Liu, Y., Gall, K., Dunn, M. L., Greenberg, A. R. & Diani, J. (2006), "Thermomechanics of shape memory polymers: Uniaxial experiments and constitutive modeling", *International Journal of Plasticity,* Vol. 22 No. 2**,** pp. 279-313.

Liu Z., Toh W., and Ng T. Y.. (2015), "Advances in Mechanics of Soft Materials: A Review of Large Deformation Behavior of Hydrogels," *International Journal of Applied Mechanics*, Vol. 7 No. 5, pp. 1530001(1-35).

Lu X., Wang C., Li G., Liu Y., Zhu X., and Tu S.. (2017), "The Mechanical Behavior and Martensitic Transformation of Porous NiTi Alloys Based on Geometrical Reconstruction," *International Journal of Applied Mechanics*, Vol. 9 No. 3, pp. 1750038

Migliavacca, F., Gervaso, F., Prosi, M., Zunino, P., Minisini, S., Formaggia, L. & Dubini, G. 2007. Expansion and drug elution model of a coronary stent. *Computer Methods in Biomechanics & Biomedical Engineering,* Vol. 10 No. 1, pp. 10-63.

Migliavacca, F., Petrini, L., Massarotti, P., Schievano, S., Auricchio, F. & Dubini, G. (2004), "Stainless and shape memory alloy coronary stents: a computational study on the interaction with the vascular wall", *Biomech Model Mechanobiol,* Vol. 2 No. 4**,** pp. 205-217.

Neamtu, I., Chiriac, A. P., Diaconu, A., Nita, L. E., Balan, V. & Nistor, M. T. (2014), "Current concepts on cardiovascular stent devices", *Mini Reviews in Medicinal Chemistry,* Vol. 14 No. 6**,** pp. 505-536.

Pan, Z. & Liu, Z. (2018), “A novel fractional viscoelastic constitutive model for shape memory polymers”, *Journal of Polymer Science Part B: Polymer Physics*, Vol. 56 No. 16, pp. 1125-1134.

Ratna, D. & Karger-Kocsis, J. (2008), "Recent advances in shape memory polymers and composites: a review", *Journal of Materials Science,* Vol. 43 No. 1**,** pp. 254-269.

Ravindranath, R. R., Romaschin, A. & Thompson, M. (2015), "In vitro and in vivo cell-capture strategies using cardiac stent technology - A review", *Clinical Biochemistry*, Vol. 49 No. 1, pp. 186-191.

Rosso, F., Marino, G., Giordano, A., Barbarisi, M., Parmeggiani, D. & Barbarisi, A. (2005), "Smart materials as scaffolds for tissue engineering", *Journal of Cellular Physiology,* Vol. 203 No. 3**,** pp. 465-470.

Small, W., Singhal, P., Wilson, T. S. & Maitland, D. J. (2010), "Biomedical applications of thermally activated shape memory polymers", *Journal of Materials Chemistry,* Vol. 20 No. 17**,** pp. 3356-3366.

Tobushi, H., Okumura, K., Hayashi, S. & Ito, N. (2001), "Thermomechanical constitutive model of shape memory polymer", *Mechanics of Materials,* Vol. 33 No. 10**,** pp. 545-554.

Volk, B. L., Lagoudas, D. C. & Maitland, D. J. (2011), "Characterizing and modeling the free recovery and constrained recovery behavior of a polyurethane shape memory polymer", *Smart Materials & Structures,* Vol. 20 No. 9**,** pp. 940041-9400418.

Wache, H. M., Tartakowska, D. J., Hentrich, A. & Wagner, M. H. (2003), "Development of a polymer stent with shape memory effect as a drug delivery system", *Journal of Materials Science Materials in Medicine,* Vol. 14 No. 2**,** pp. 109-112.

Wang, Q., Fang, G., Zhao, Y., Wang, G. & Cai, T. (2016), "Computational and experimental investigation into mechanical performances of Poly-L-Lactide Acid (PLLA) coronary stents". *Journal of the Mechanical Behavior of Biomedical Materials,* Vol. 65**,** pp. 415-427.

Wang, R., Zuo, H., Yang, Y. M., Yang, B. & Li, Q. (2017), "Finite element simulation and optimization of radial resistive force for shape memory alloy vertebral body stent", *Journal of Intelligent Material Systems & Structures,* Vol. 15 No. 28**,** pp. 2140-2150.

Yakacki, C. M., Shandas, R., Lanning, C., Rech, B., Eckstein, A. & Gall, K. (2007), "Unconstrained Recovery Characterization of Shape-Memory Polymer Networks for Cardiovascular Applications", *Biomaterials,* Vol. 28 No. 14**,** pp. 2255-2263.

Yu, K. & Qi, H. J. (2014), "Temperature memory effect in amorphous shape memory polymers", *Soft Matter,* Vol. 10 No. 47, pp. 9423-9432.

Zheng, S., Li, Z. & Liu, Z. (2018), "The fast homogeneous diffusion of hydrogel under different stimuli", *International Journal of Mechanical Sciences,* Vol. 137**,** pp. 263-270.

©Corresponding author
Zishun Liu can be contacted at: zishunliu@mail.xjtu.edu.cn